

# We are IntechOpen, the world's leading publisher of Open Access books Built by scientists, for scientists

4,800

Open access books available

122,000

International authors and editors

135M

Downloads

Our authors are among the

154

Countries delivered to

TOP 1%

most cited scientists

12.2%

Contributors from top 500 universities



WEB OF SCIENCE™

Selection of our books indexed in the Book Citation Index  
in Web of Science™ Core Collection (BKCI)

Interested in publishing with us?  
Contact [book.department@intechopen.com](mailto:book.department@intechopen.com)

Numbers displayed above are based on latest data collected.  
For more information visit [www.intechopen.com](http://www.intechopen.com)



# Effective Low Frequency Noise Insulation Adopting Active Damping Approaches

*Ming Yuan and Fan Yang*

## Abstract

In this chapter, effective low frequency noise insulation adopting active damping approaches are illustrated. In general, engineering plate structures suffer insufficient noise insulation performance in the low frequency band. To improve the structure's noise insulation performance, active damping methods can be utilized, which aim to suppress plate structure's efficient sound radiation modes. The collocated sensor/actuator configuration guarantees the control system's robustness, and simplifies the control law design. In the presented study, two control laws are proposed to add active damping to the structure. One control law is negative acceleration feedback (NAF) control and the other control law is filtered velocity feedback (FVF) control. The NAF control is suitable to control one specific mode and the FVF control is suitable to realize wide band vibration control. With respect to practical implementation, a carbon fiber reinforced plastic (CFRP) plate is served as the control target and active control laws are implemented on it. Experimental system for active control is presented in detail, and some practical advises are given to help readers to solve similar problems in a convenient way. The measured sound pressure and vibration results show effectiveness of the active damping treatment.

**Keywords:** noise insulation, low frequency, active damping, control laws, smart structure, real-time control

## 1. Introduction

Low frequency noise and vibration control has always been hot spot in academic and industry fields. For examples, in aircraft, vehicles, trains and industrial machines, large amplitude of structural responses are fluent in the low frequency ranges. These unwanted disturbances give rise to large decibels of noise and accelerating structure fatigue. Meanwhile, the noise's detrimental effect to human being's health has been well known [1].

In the mentioned examples above, plate structures are widely used. In general, the plate's structural parameters have been determined in advance, and lightweight structure is favorable for cost reduction. Accordingly, the plate structure usually have small thickness and low damping characteristics. When external noise excites the plate structure, the plate itself becomes an effective sound transmission path to the internal space [2, 3]. Specially, when the excitation frequency equals to the

plate structure's natural frequency, large amplitude of vibration can impetus air particles strongly, making the structure itself can radiate noise efficiently [4].

To improve the plate's noise insulation performance, special treatments should be adopted to attenuate the sound transmission. An effective approach is adding damping to the plate. Accordingly, the structural vibration response is reduced, which can improve the structure's sound insulation performance substantially.

Among the damping approaches, passive damping is a simple and effective approach to realize vibration control. For instance, the viscoelastic material based approach has been applied widely in the engineering applications. However, this approach is only suitable to the mid-high frequencies and does not have satisfying performance in the low frequency range [5], especially when the installation have rigorous restrictions of added weight and spaces.

In another vein, active damping approaches have shown to be a good candidate to realize effective vibration control in the low frequency range. To perform active damping, an active control system is needed, which requires power supply. A classical active control system is composed by sensor, actuator, signal conditioner, controller and power amplifier [6].

In this study, we adopt piezoelectric smart material to realize structural sensing and actuating functions. The piezoelectric material can be integrated into the structure easily, which requires little mounting spaces [7]. The piezoelectric effect enables the structural signal being converted into electrical signal, and accelerometer is a commercialized product. The inverse piezoelectric effect enables the piezoelectric material being adopted as actuator, which follows the control signal well in the low frequency range. With proper design, it is anticipated that the plate's noise insulation performance can be improved significantly in the low frequency range after active control.

In Section 2, the general structural dynamic properties are characterized, and the interesting modes to be controlled are refined; in Section 3, the active control laws are proposed to increase the structure's damping behavior; in Section 4, some practical implementation issues for the active system are emphasized; in Section 5, a CFRP plate is selected as the control target and the performance of active sound insulation is evaluated.

## 2. Frequency band classification and interesting target modes

### 2.1 Frequency band classification

In general, the frequency range of the structural dynamics can be classified into three frequency bands, i.e., low frequency, mid frequency and high frequency [8, 9].

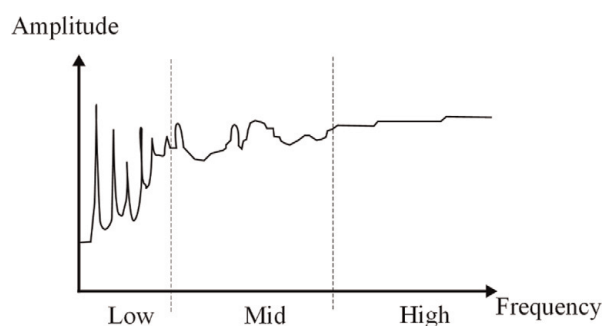


**Figure 1.**  
*Frequency band classification based on modal overlapping.*

As shown in **Figure 1**, in the low frequency band, the structural responses are characterized by apparent vibration modes, peaks and troughs can be found at the corresponding frequency response plot. Besides, the structural uncertainties are small, making the structure's vibro-acoustic behavior can be predicted well with the help of finite element method.

When the frequency goes up into the mid and high frequency range, the modal overlapping increases and the peaks and troughs cannot be distinguished clearly from the frequency response plot. Meanwhile, the structural uncertainties and computation burden increase intensively, causing the finite element method being not suitable to handle such problem.

## 2.2 Interesting target modes

To realize effective active sound insulation, the vibration modes to be controlled must be selected carefully. Because the sound excitation is wideband in general, indicating multiple vibration modes can be excited at the same time, which brings difficulty to the control law design. Luckily, for each vibration mode, its sound radiation effectiveness differs significantly. If some modes contribute little to the far-field sound field, these modes can be omitted in the active control law design.

Besides, the mode selection has close relationship to the control loop's sensor/actuator placement. In general, the measured sensing signal should have sufficient signal to noise ratio (SNR) value. If the sensor/actuator is not placed properly, the control law's effectiveness and robustness will be decreased, owing to the low SNR value.

To place the sensor/actuator properly, and identify the interesting target modes, modal analysis can be adopted. Here, a rectangular plate is illustrated as an example and its first four mode shapes are presented in **Figure 2**.

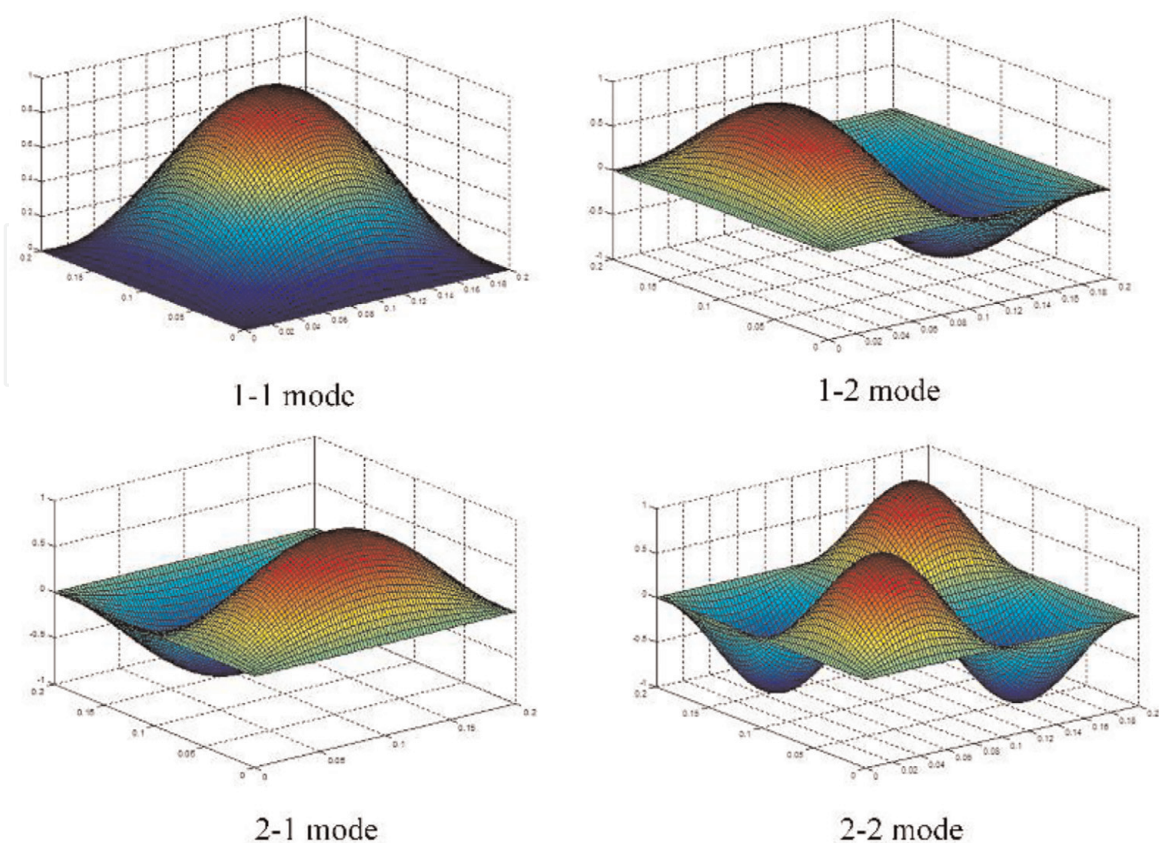


**Figure 2.**  
*Vibration mode shapes of rectangular plate.*

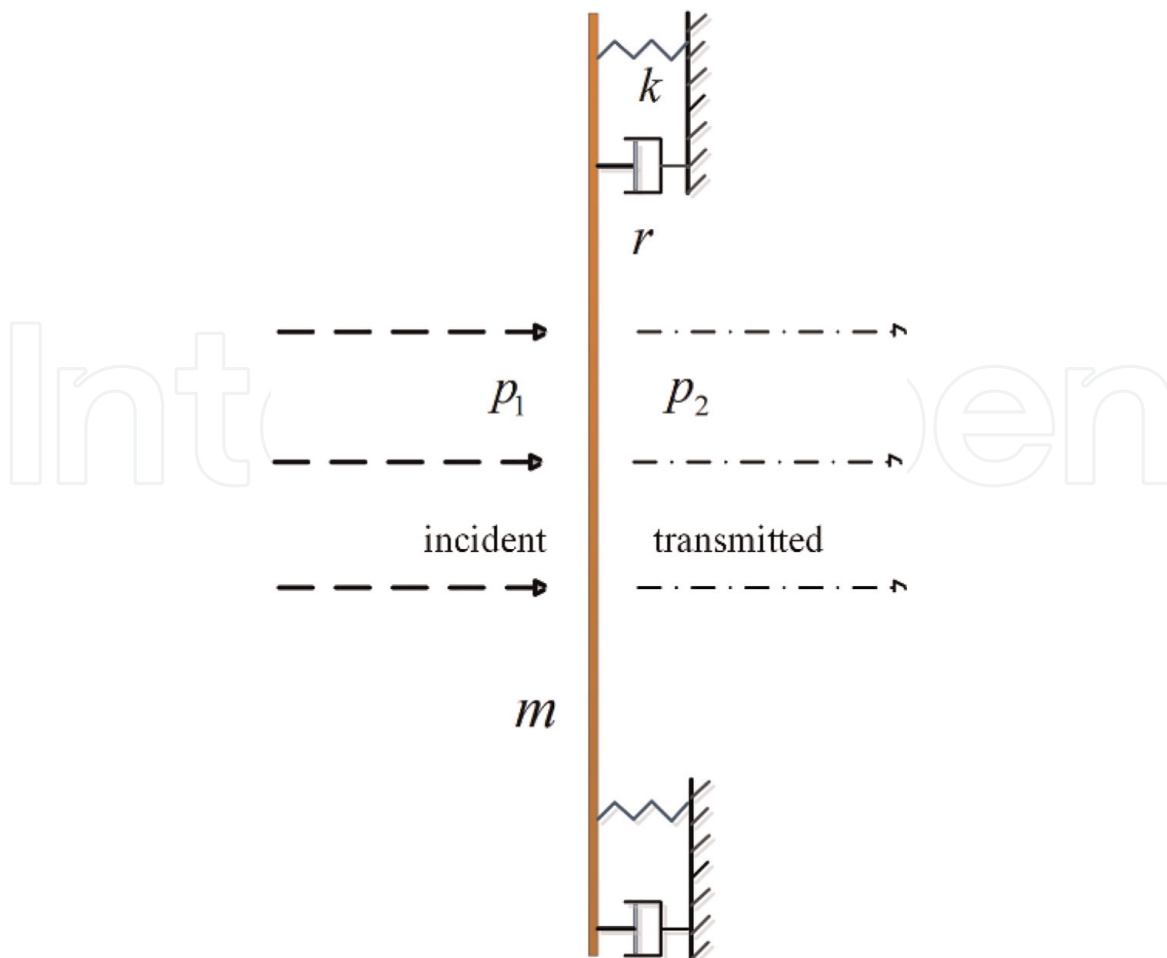


**Figure 3.**  
Simplified model for noise insulation study.

According to these mode shapes, it is shown that the 2-2 mode (even-even mode) shape radiates like a quadrupole acoustic source. In the low frequency range, for such vibration mode, the neighboring push-pull phenomenon makes acoustic cancellation occurs strongly. Similarly, acoustic cancellation also occurs strongly at the 1-2 mode (odd-even mode) and 2-1 mode (even-odd mode), which reduce these modes' sound radiation effectiveness. The 1-1 mode (odd-odd mode) radiates like a monopole, which has the highest sound radiation ability.

Furthermore, the mode's radiation efficiencies can be quantized with different boundary conditions. For the simply supported boundary, the detailed equations can be found in Refs. [10, 11]. For the clamped boundary, the detailed equations can be found in Ref. [12].

These above analysis indicates that in the active sound insulation application, the main interested modes will be odd-odd modes. At the resonant frequency, and assuming the displacement is uniform, the structure can be simplified into a dynamic system with one degree of freedom.

As shown in **Figure 3**, the sound pressure from the incident side is  $p_1$  and the sound pressure from the transmitted side is  $p_2$ . The structural displacement is  $\eta$ , damping coefficient is  $r$ , stiffness coefficient is  $k$ , the dynamic system can be expressed as:

$$m\ddot{\eta} + r\dot{\eta} + k\eta = p_1 - p_2 \quad (1)$$

The volume velocity is assumed continuous at the plate's two sides, and the corresponding acoustic impedance is:

$$Z = (p_1 - p_2)/\dot{\eta} = j\omega m \left( 1 - \frac{\omega_0^2}{\omega^2} \right) + r \quad (2)$$

where  $\omega_0 = \sqrt{k/m}$  is the natural frequency.

According to the definition of sound transmission loss, when the incident sound wave is in vertical direction of the structure, the noise insulation metric can be calculated as:

$$\begin{aligned} R &= 10 \log_{10} \left| \frac{p_1}{p_2} \right|^2 = 10 \log_{10} \left| 1 + \frac{Z}{2\rho_0 c_0} \right|^2 \\ &= 10 \log_{10} \left| 1 + \frac{j\omega m \left( 1 - \frac{\omega_0^2}{\omega^2} \right) + r}{2\rho_0 c_0} \right|^2 \end{aligned} \quad (3)$$

where  $\rho_0 c_0$  is the air's characteristic impedance.

The noise insulation suffers the lowest value at the resonant frequency, which can be expressed as:

$$R = 10 \log_{10} \left| 1 + \frac{r}{2\rho_0 c_0} \right|^2 \quad (4)$$

As shown in Eq. (4), to improve the noise insulation performance, the damping should be increased.

### 3. Active noise insulation control laws

#### 3.1 Sensor and actuator placement

From the control engineering's perspective, sensor/actuator selection and placement correlate to the system's observability and controllability. For instance, for an interesting mode, if the sensor is placed at the structure's nodal point, no informative response can be obtained. The measured signal is buried in noise. Similarly, if the actuator is placed along the interesting mode's nodal line, this mode will be uncontrollable.

To improve the control law's robustness and facilitate control law design, the collocated sensor/actuator configuration is favorable. Under such configuration, the transmission path between the collocated actuator and sensor is the nearest, generates a minimum phase system. In other words, the magnitude and phase responses between the sensor and actuator is unique and the pole/zero appears in an interlacing way. Correspondingly, as shown in **Figure 4**, the resonant peaks and anti-resonant trough will appear one by one. In the phase plot,  $180^\circ$  phase lag is generated across the resonant frequency and  $180^\circ$  phase lead is generated across the anti-resonant frequency. If the two adjacent modes are near, the modes' coupling makes the phase lag being smaller than  $180^\circ$ . In summary, the interlacing property makes the phase lag's variation always within  $180^\circ$ , which facilitates the control law design.

In practical implementation, the sensor and actuator's physical properties make the collocation in a limited frequency range. This means the phase lag between the sensor/actuator pair will beyond  $180^\circ$  above certain frequency limit. Therefore, to meet the Nyquist criterion [13], the controller's gain must be limited within a certain range.

### 3.2 Negative acceleration feedback (NAF) control

The NAF control law utilize the structural acceleration signal as the input signal. Then the control output is generated according to the NAF control law, which is written as:

$$H_{NAF}(j\omega) = g \frac{\omega_c^2}{-\omega^2 + 2\omega_c\zeta_{NAF}j\omega + \omega_c^2} \quad (5)$$

where  $g$  is the control gain,  $\omega_c$  is the targeting control angular frequency,  $\zeta_{NAF}$  is the controller's damping ratio parameter.

According to the analysis given in [14], at the targeting control angular frequency, the NAF control law generates active damping to the structure.

For a given control frequency, with different control damping parameters, the NAF controller's bode plot values is shown in **Figure 5**.

The damping ratio value should be paid attention for practical implementation. Clearly, if a lower damping ratio value is adopted, the control authority will be

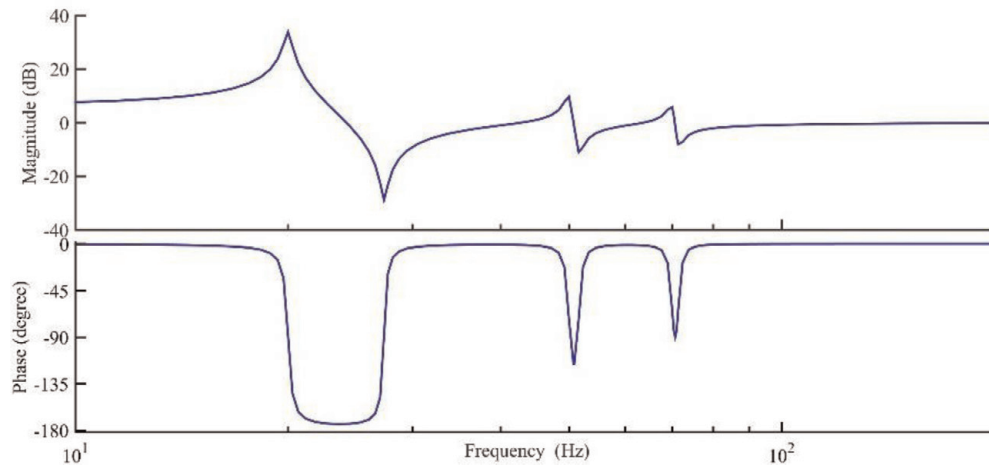


**Figure 4.**  
*Interlacing property of the collocated sensor/actuator configuration.*

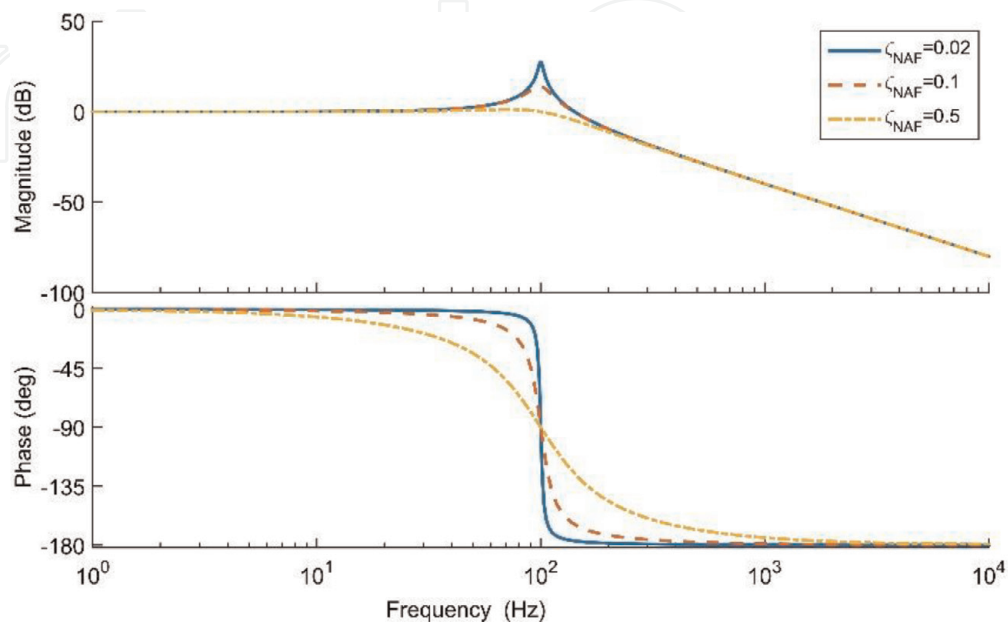


**Figure 5.**  
*Bode plot of the NAF controller with different control damping ratio parameters.*

increased for a certain frequency. Because the controller can generate larger output at this frequency. However, the control performance will be reduced substantially when the target frequency is slightly biased from the realistic resonant frequency. If the damping value is too large, the control authority will be weak, and the added active damping effectiveness will be small.

The merit of NAF controller is: the control authority is exerted to one specific mode. The controller rolls-off at 40 dB/dec above the target control frequency. This roll-off characteristic can suppress high frequency noise effectively, which is favorable to guarantee the control gain.

Concerning multiple modes suppression, the same number of NAF controllers will be needed and the NAF controllers should be connected in parallel. However, the authors do not recommend using NAF control law to suppress more than three modes. One important reason is, when the interesting modes are adjacent, because the controller's output does not rolling off sufficiently, the control interferences are generated, making the control law's tuning process being complicated.

### 3.3 Filtered velocity feedback (FVF) control

Direct velocity feedback (DVF) control utilizes the structural velocity as the feedback signal directly. The controller is a constant gain, which can generate active damping to the structure [15].

Because the DVF control law does not provide roll-off property, the control authority is limited for practical experimental test. However, in the sound insulation application, to realize global reduction, wideband active damping is required essentially.

To fulfill this task, the DVF control law must be modified and Filtered Velocity Feedback (FVF) control is proposed to improve the control performance. The FVF control law behaves like an electrical dynamic absorber, which can be deduced according to Ref. [16].

In the frequency domain, the FVF controller can be expressed as:

$$H_{FVF}(j\omega) = g \frac{j\omega + 2\omega_n \zeta_{FVF}}{-\omega^2 + 2\omega_n \zeta_{FVF} j\omega + \omega_n^2} \quad (6)$$

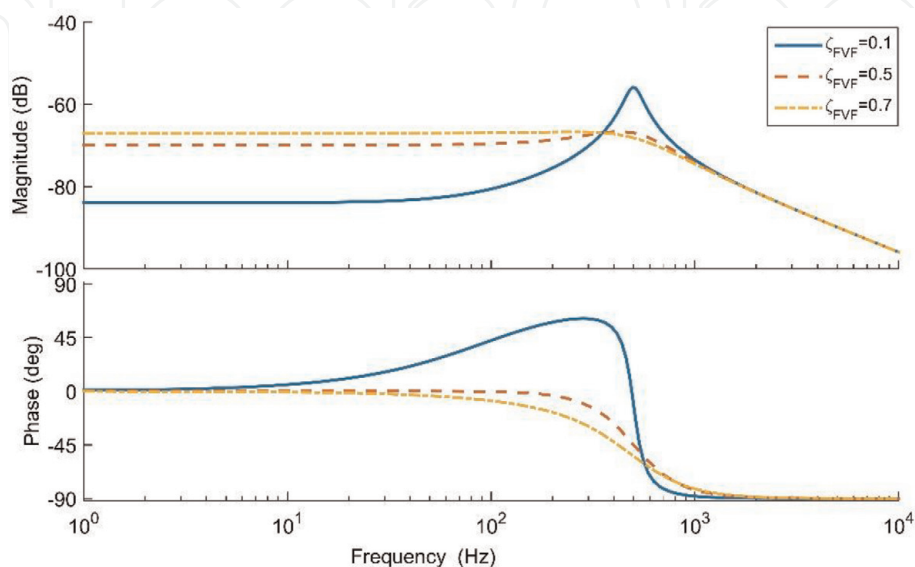


**Figure 6.**  
 Bode plot of the FVF controller with different control damping ratio parameters.



where  $g$  is the control gain,  $\omega_n$  is the controller's upper frequency,  $\zeta_{FVF}$  is the controller's damping ratio.

For a given control frequency, the FVF controller's Bode plot with different control damping values is shown in **Figure 6**.

As shown in **Figure 6**, in the low frequency, the controllers behaves like a DVF controller but the control output rolls off at 20 dB/dec after the controller's upper frequency. Therefore, active damping is generated in the low frequency range.

Unlike the NAF controller, the damping ratio of FVF controller should be high enough to generate sufficient gain below the upper frequency. For instance,  $\zeta_{FVF} = 0.7$  is a good choice.

If acceleration signal is used as the control input instead of velocity signal, the modified FVF control law becomes into:

$$H'_{FVF}(j\omega) = g \frac{j\omega + 2\omega_n \zeta_{FVF}}{j\omega(-\omega^2 + 2\omega_n \zeta_{FVF} j\omega + \omega_n^2)} \quad (7)$$

## 4. Implementation considerations

### 4.1 Real-time control platform

To implement the control law, a real-time operating system (RTOS) is required to maintain the control law operating in a deterministic way. Normally, the sensing signal is sampled from the analog input channel, and the data acquisition device is switched to hardware-timed single point mode. The real-time control system guarantees the control law being updated within the period of two consecutive sampling points. After the control algorithm is updated, the output signal is sent to the analog output channel.

In general, the control law's thread should have the highest priority during the execution. This mechanism makes the control law can be implemented in a deterministic way. The other functions of the RTOS, such as signal monitoring, data logging and network communications are usually assigned to low execution priorities.

For rapid control system prototyping, some examples of the real-time target are: PXI target [17], CompactRIO target [18], Speedgoat target [19] and dSPACE target [20]. These real-time platforms' corresponding photo is shown in **Figure 7**.

### 4.2 Delay minimization

With respect to the feedback control system, time delay is highly unwanted. However, inside the feedback control system, each component can introduce some kind of delay, which generates adverse influence to system's stability and performance.

For a pure delay system, the phase lag (in degree) can be expressed as:

$$\varphi = -57.3 \times \omega \times T \quad (8)$$

where  $\omega$  is the angular frequency and  $T$  is the time caused by system delay.

If the sensor and actuator are placed in the collocated configuration, the physical signal's propagation delay from the actuator to the sensor is minimized. Therefore, the digital control system becomes the primary time delay source, which has close relationship with the sampling rate.

To minimize the delay caused by data sampling, the sampling rate should be high enough. In general, the sample rate should be at least 10 times higher than the

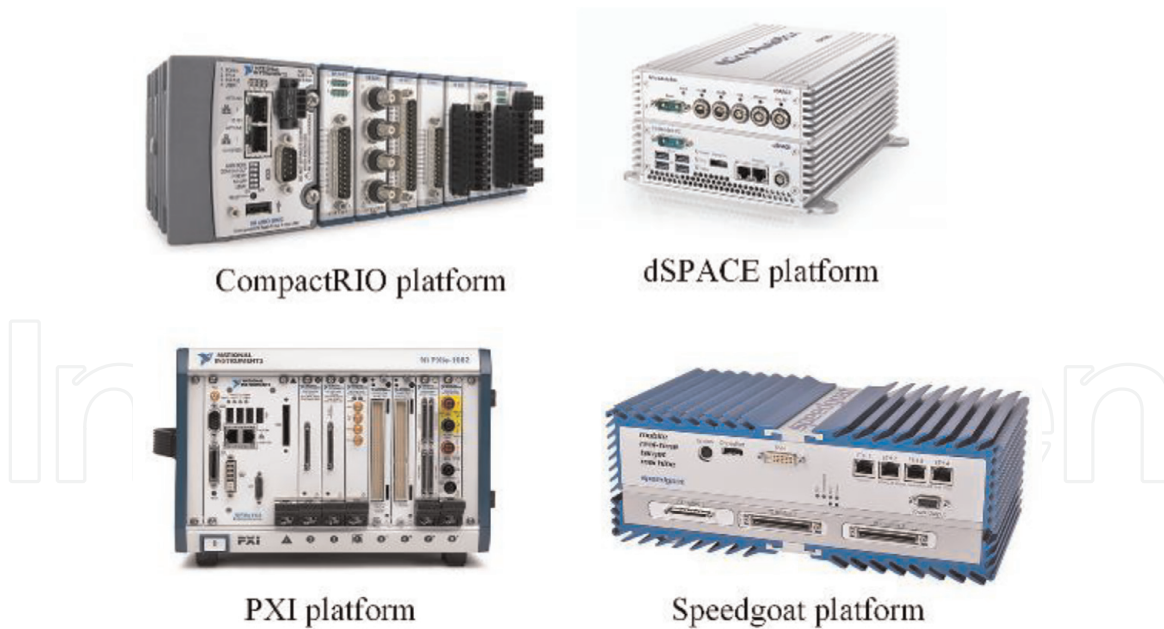


**Figure 7.**  
*Real-time control platforms for rapid prototyping.*

interesting bandwidth's upper frequency. However, the achieved sampling rate is also restricted by the controller. When the control law requires intensive computation effort and the controller is not fast enough, the control law will not be finished in time. In such circumstance, to meet the deterministic mechanism, the sampling rate should be reduced.

In summary, to determine the control law's updating rate, the control bandwidth, computation burden and real-time target's performance should be taken into consideration simultaneously.

### 4.3 Filter

Filters are widely used in active control systems, which can suppress excessive noise signal. Crucially, if the control law itself does not have the roll-off characteristic in the high frequency, low pass filter will be always favorable. The high pass filter can also be utilized to suppress the ultra-low frequency noise.

The filter's cut-off frequency and order should be determined with respect to the control plant. For the realization form, analog filter is recommended. Because analog filter has much less propagation delay than the digital filter.

## 5. Case studies

As shown in **Figure 8**, the sound insulation test was performed in an anechoic room. The control target is a stiffened CFRP plate and the dimension parameter is  $840 \text{ mm} \times 840 \text{ mm} \times 1 \text{ mm}$ . The plate is mounted on an aluminum cavity, with a thickness of 16 mm. A loudspeaker is placed inside the cavity, which generates acoustic excitation the stiffened plate. The CFRP plate is clamped to the aluminum cavity using screws. The edges between the CFRP plate and aluminum box are sealed to prohibit air leakage.

According to the sound insulation mass law, because the box's thickness is much larger than the CFRP plate, the sound transmission path from the internal cavity to

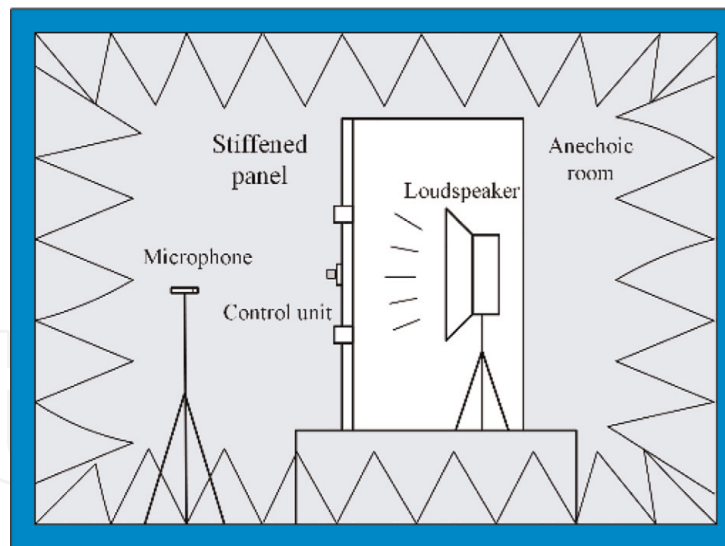


**Figure 8.**  
*Schematic diagram for the active sound insulation test.*

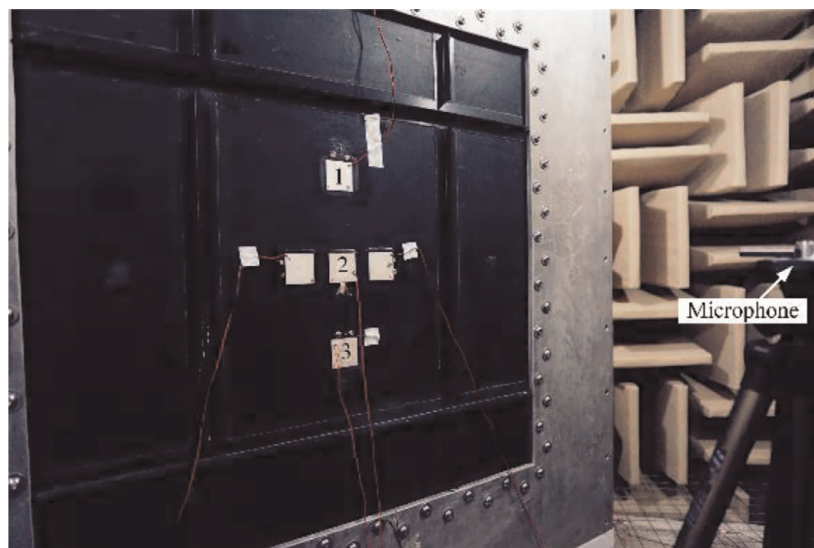


**Figure 9.**  
*Photograph of the test structure.*

the outside is the latter. To evaluate the control law's performance, in front of the CFRP plate, a microphone sensor (G.R.A.S 40 ph) is used to monitor the sound pressure level (SPL) value. The distance between the microphone sensor and CFRP plate is 1 m.

For the control system implementation, three independent control channels are adopted. Correspondingly, as shown in **Figure 9**, three piezoelectric PZT-5H patches are served as actuators, which are labeled as 1, 2, 3.

The detailed components of control system are shown in **Figure 10**. Collocated accelerometers are bonded to the central of the piezoelectric patches, which are used for structural sensing. Control algorithms are programmed using LabVIEW™ and subsequently compiled and downloaded into a CompactRIO target for real-time implementation. A Virtex-5 LX110 FPGA chip guarantees the control loops can be implemented with high throughput and in parallel physically [21].

The digital control loop's updating rate is set to 20 kHz. To transform the continuous transfer function into discretized form, bilinear transformation method is adopted. The equation of the bilinear transformation is shown as follows:

$$z = \frac{1 + Ts/2}{1 - Ts/2} \quad (9)$$

where  $T$  is the sampling time.

The components of the control system is shown in **Figure 10**. Band-limited noise (20–500 Hz) is sent to the loudspeaker, which can excite multiple vibration modes of the CFRP panel. Besides, the 1-1 mode is a global vibration mode, which needs more control effort. In view of the above circumstances, a hybrid control law is proposed to solve the problem.

In the hybrid scheme, the NAF control puts control authority to the plate's 1-1 mode and FVF control puts control authority to multiple modes of the plate.

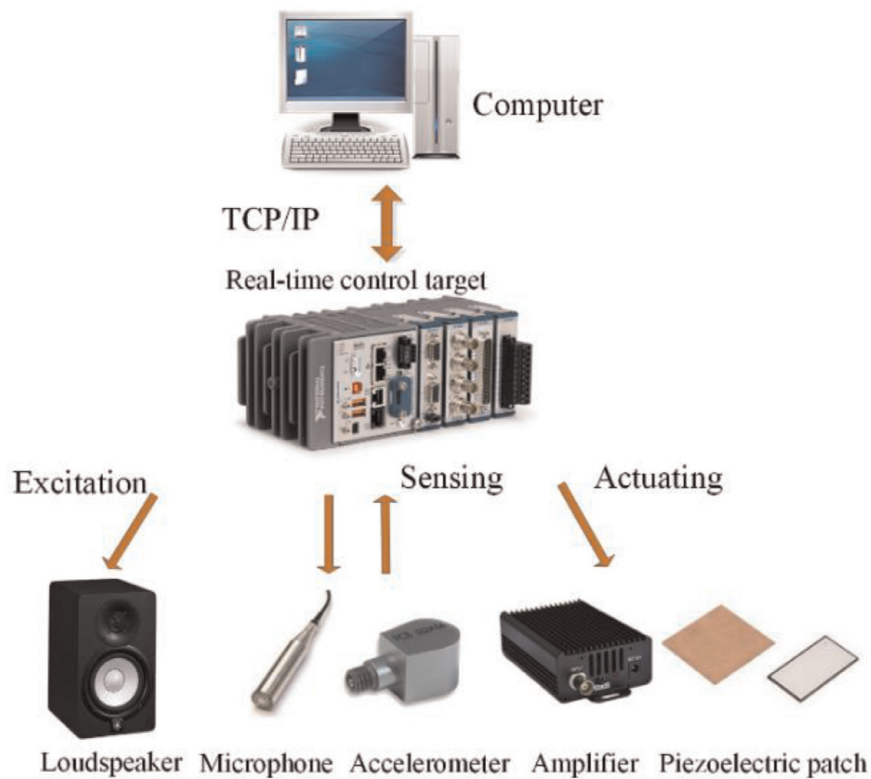


**Figure 10.**  
 Components of the control system.

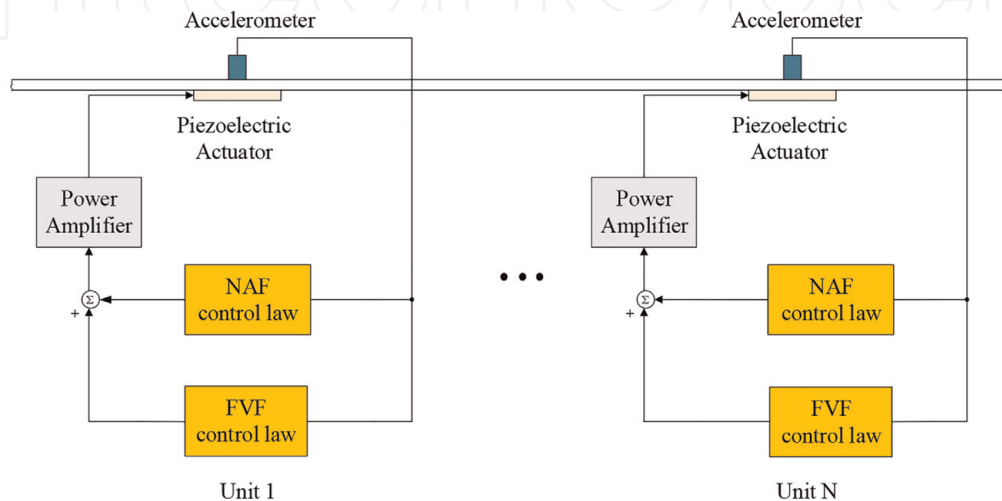


**Figure 11.**  
 Schematic diagram of the hybrid control system.

Therefore, it is anticipated that this hybrid control law can exert sufficient active damping to the CFRP panel, which is suitable for the noise insulation application.

The schematic diagram of the hybrid control system is shown **Figure 11**.

When the active insulation system starts to work, the acceleration signal spectrums before control and after control are shown in **Figure 12**.

From the measured data, the proposed hybrid control scheme can realize wideband vibration reduction. For instance, at 83 Hz, the vibration reduction value is 13 dB; at 143 Hz, the vibration reduction value is 6.6 dB; at 194 Hz, the vibration reduction value is 5.3 dB; at 216 Hz, the vibration reduction value is 5.2 dB; at 273 Hz, the vibration reduction value is 4.3 dB; at 305 Hz, the vibration reduction value is 5.9 dB.

The SPL spectrums before control and after control are shown in **Figure 13**.

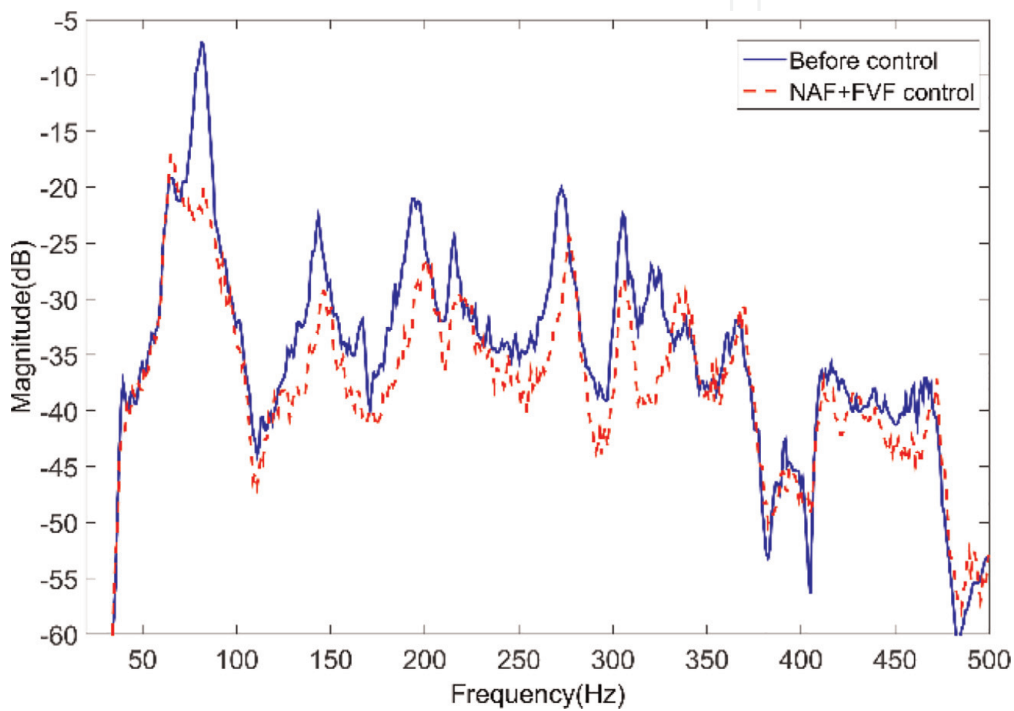


**Figure 12.**  
Measured acceleration signal (solid line: before control, dashed line: after control).

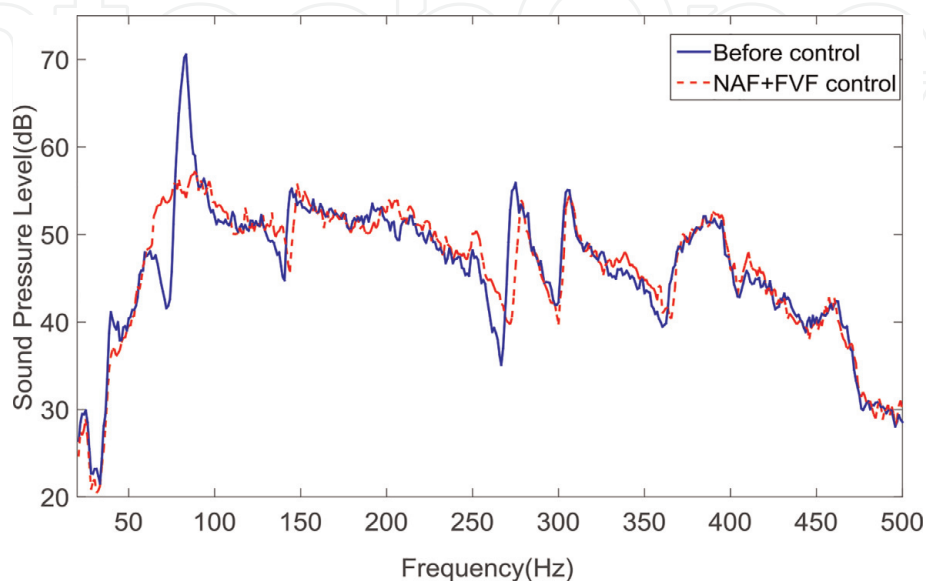


**Figure 13.**  
Measured sound pressure level (solid line: without control, dashed line: with control).

At 83 Hz, as anticipated, this first vibration mode contribute to the SPL spectrum significantly. After the active damping treatment, at this frequency, the SPL reduction value is up to 15.3 dB. For the entire interesting frequency band, the SPL reduction value comes up to 7.3 dB. These measured experimental results prove that the proposed active damping control method can improve the structure's sound insulation performance in an effective way.

## 6. Conclusions

In this chapter, the active damping approaches are adopted to improve structure's sound insulation performance in the low frequency range. The collocated sensor/actuator configuration is adopted to simplify the control law design. The NAF control law is proposed to suppress the plate's 1-1 mode, which radiates sound effectively and needs more control authority. The FVF control is proposed to suppress multiple vibration modes in wide range. In the experimental study, a CFRP panel is utilized as the control target and the NAF and FVF control laws are combined together to generate active damping to the CFRP structure. Experimental test results show the hybrid control law can realize wideband active damping and improve the plate's sound insulation performance significantly.

## Acknowledgements

This work was funded by the National Natural Science Foundation of China (grant numbers 61701250, 51605202), the Natural Science Foundation of Jiangsu Province (grant number BK20160895, BK20160550).

## Conflict of interest

The authors declare no conflict of interest.

## Author details


Ming Yuan<sup>1\*</sup> and Fan Yang<sup>2\*</sup>

<sup>1</sup> School of Automation, Nanjing University of Posts and Telecommunications, Nanjing, China

<sup>2</sup> School of Naval Architecture and Ocean Engineering, Jiangsu University of Science and Technology, Zhenjiang, China

\*Address all correspondence to: [yuanming@njupt.edu.cn](mailto:yuanming@njupt.edu.cn) and [yangf@just.edu.cn](mailto:yangf@just.edu.cn)

## IntechOpen

© 2019 The Author(s). Licensee IntechOpen. This chapter is distributed under the terms of the Creative Commons Attribution License (<http://creativecommons.org/licenses/by/3.0>), which permits unrestricted use, distribution, and reproduction in any medium, provided the original work is properly cited. 

## References

- [1] Ising H, Kruppa B. Health effects caused by noise: Evidence in the literature from the past 25 years. *Noise & Health* [Internet]. 2004;**6**(22):5-13. Available from: <http://www.noiseandhealth.org/article.asp?issn=1463-1741>
- [2] Wilby JF. Aircraft interior noise. *Journal of Sound and Vibration*. 1996; **190**(3):545-564
- [3] Yuan M, Ohayon R, Qiu J. Decentralized active control of turbulent boundary induced noise and vibration: A numerical investigation. *Journal of Vibration and Control* [Internet]. 2016;**22**(18):3821-3839. DOI: 10.1177/1077546314566441
- [4] Fahy FJ, Gardonio P. *Sound and Structural Vibration: Radiation, Transmission and Response*. Oxford: Academic Press; 2007
- [5] Baz AM. *Active and Passive Vibration Damping*. 1st ed. Hoboken, NJ, USA: Wiley; 2019. pp. 1-5
- [6] Yuan M, Ji H, Qiu J, Ma T. Active control of sound transmission through a stiffened panel using a hybrid control strategy. *Journal of Intelligent Material Systems and Structures* [Internet]. 2012;**23**(7):791-803. DOI: 10.1177/1045389X12439638
- [7] Wang Y, Inman DJ. A survey of control strategies for simultaneous vibration suppression and energy harvesting *via* piezoceramics. *Journal of Intelligent Material Systems and Structures*. 2012;**23**(18):2021-2037
- [8] Morand HJ-PP, Ohayon R. *Fluid Structure Interaction*. New York: John Wiley; 1995. 212 p
- [9] Ohayon R, Soize C. *Advanced Computational Vibroacoustics: Reduced-Order Models and Uncertainty Quantification*. New York: Cambridge University Press; 2014. pp. 1-127
- [10] Wallace CE. Radiation resistance of a rectangular panel. *The Journal of the Acoustical Society of America* [Internet]. 1972;**51**(3B):946-952. DOI: 10.1121/1.1912943
- [11] Pierre RLS Jr, Koopmann GH, Chen W. Volume velocity control of sound transmission through composite panels. *Journal of Sound and Vibration*. 1998; **210**(4):441-460
- [12] Berry A, Guyader J, Nicolas J. A general formulation for the sound radiation from rectangular, baffled plates with arbitrary boundary conditions. *The Journal of the Acoustical Society of America*. 1990;**88**(6): 2792-2802
- [13] Franklin GF, Powell JD, Naeini AE. *Feedback Control of Dynamic Systems*. 7th ed. Upper Saddle River, New Jersey: Pearson Press; 2015
- [14] Yuan M, Qiu J, Ji H, Zhou W, Ohayon R. Active control of sound transmission using a hybrid/blind decentralized control approach. *Journal of Vibration and Control* [Internet]. 2013;**21**(13):2661-2684. DOI: 10.1177/1077546313514758
- [15] Balas MJ. Direct velocity feedback control of large space structures. *Journal of Guidance, Control, and Dynamics* [Internet]. 1979;**2**(3):252-253. DOI: 10.2514/3.55869
- [16] Yuan M. Compact and efficient active vibro-acoustic control of a smart plate structure. *International Journal of Engineering*. 2016;**29**(8):1068-1074
- [17] PXI Systems [Internet]. Available from: <http://www.ni.com/en-us/shop/pxi.html>

[18] CompactRIO Systems [Internet].  
Available from: <http://www.ni.com/en-us/shop/compactrio.html>

[19] Speedgoat Systems [Internet].  
Available from: <https://www.speedgoat.com/>

[20] dSPACE Systems [Internet].  
Available from: [https://www.dspace.com/shared/data/pdf/2018/dSPACE\\_Systems.pdf](https://www.dspace.com/shared/data/pdf/2018/dSPACE_Systems.pdf)

[21] Yuan M. Field programmable gate Array implementation of active control laws for multi-mode vibration damping. *International Journal of Engineering-Transactions B: Applications*. 2016; **29**(2):229-235

IntechOpen